



A framework for expanding aqueous chemistry in the Community Multiscale Air Quality (CMAQ) model version 5.1

Kathleen M. Fahey¹, Annmarie G. Carlton², Haval O. T. Pye¹, Jaemeen Baek^a, William T. Hutzell¹, Charles O. Stanier³, Kirk R. Baker⁴, K. Wyatt Appel¹, Mohammed Jaoui⁵, and John H. Offenberg⁵

¹Computational Exposure Division, National Exposure Research Laboratory, Office of Research and Development, US Environmental Protection Agency, Research Triangle Park, NC, USA

²Department of Chemistry, University of California, Irvine, Irvine, CA, USA

³Department of Chemical and Biochemical Engineering, University of Iowa, Iowa City, IA, USA

⁴Air Quality Assessment Division, Office of Air Quality Planning and Standards, Office of Air and Radiation, US Environmental Protection Agency, Research Triangle Park, NC, USA

⁵Exposure Methods and Measurements Division, National Exposure Research Laboratory, Office of Research and Development, US Environmental Protection Agency, Research Triangle Park, NC, USA

^aformerly at: Department of Chemical and Biochemical Engineering, University of Iowa, Iowa City, IA, USA

Correspondence to: Kathleen M. Fahey (fahey.kathleen@epa.gov)

Received: 29 November 2016 – Discussion started: 8 December 2016

Revised: 2 March 2017 – Accepted: 10 March – Published: 13 April 2017

Abstract. This paper describes the development and implementation of an extendable aqueous-phase chemistry option (AQCHEM – KMT(I)) for the Community Multiscale Air Quality (CMAQ) modeling system, version 5.1. Here, the Kinetic PreProcessor (KPP), version 2.2.3, is used to generate a Rosenbrock solver (Rodas3) to integrate the stiff system of ordinary differential equations (ODEs) that describe the mass transfer, chemical kinetics, and scavenging processes of CMAQ clouds. CMAQ's standard cloud chemistry module (AQCHEM) is structurally limited to the treatment of a simple chemical mechanism. This work advances our ability to test and implement more sophisticated aqueous chemical mechanisms in CMAQ and further investigate the impacts of microphysical parameters on cloud chemistry.

Box model cloud chemistry simulations were performed to choose efficient solver and tolerance settings, evaluate the implementation of the KPP solver, and assess the direct impacts of alternative solver and kinetic mass transfer on predicted concentrations for a range of scenarios. Month-long CMAQ simulations for winter and summer periods over the US reveal the changes in model predictions due to these cloud module updates within the full chemical transport model. While monthly average CMAQ predictions are not drastically altered be-

tween AQCHEM and AQCHEM – KMT, hourly concentration differences can be significant. With added in-cloud secondary organic aerosol (SOA) formation from biogenic epoxides (AQCHEM – KMTI), normalized mean error and bias statistics are slightly improved for 2-methyltetrols and 2-methylglyceric acid at the Research Triangle Park measurement site in North Carolina during the Southern Oxidant and Aerosol Study (SOAS) period. The added in-cloud chemistry leads to a monthly average increase of 11–18 % in “cloud” SOA at the surface in the eastern United States for June 2013.

1 Introduction

Clouds and fogs impact the amount, composition, and spatial distribution of trace atmospheric species through a complex interplay of chemistry and physics. Pollutants are transported via convection and wet deposition (Barth et al., 2001; Wonaschuetz et al., 2012; Yin et al., 2001) and altered through condensed-phase chemistry (Graedel and Weschler, 1981; Lelieveld and Crutzen, 1991). Water droplets offer a medium for soluble gases to dissolve, dissociate, and undergo aqueous-phase chemical reactions. This is well established for the conversion of gas-phase SO₂ to particle-phase

sulfate (SO_4^{2-}) (Martin, 1984; Martin and Good, 1991). Atmospheric SO_4^{2-} is an important component of fine aerosol mass and is a known contributor to adverse effects on human health and ecosystems. In an environment where clouds or fogs are present, aqueous-phase production of SO_4^{2-} in cloud and fog droplets dominates over production in the gas phase (Seigneur and Saxena, 1988; Ervens, 2015), and decades of research have been devoted to studying the impacts of in-cloud production of acidic species, like SO_4^{2-} , on acid deposition, including effectively representing this in-cloud production in models (Chang et al., 1987; Walcek and Taylor, 1986; Pandis and Seinfeld, 1989; Fahey and Pandis, 2001; Gong et al., 2011; Giulianelli et al., 2014; Herckes et al., 2015). More recent studies have focused on the potentially significant role that aqueous pathways (in cloud droplets and wet aerosols) may have on the formation of secondary organic aerosol (SOA) (McNeill et al., 2012; Ervens et al., 2014, 2011; Lim et al., 2005; Liu et al., 2012; Carlton et al., 2008). It has been proposed that cloud water provides a medium for the production of highly oxidized organic compounds that remain in the aerosol phase after cloud droplet evaporation, contributing to secondary organic aerosol mass (Ervens et al., 2011; McNeill, 2015; Ervens, 2015). Sulfate and organic components can contribute more than half of the total fine particulate matter ($\text{PM}_{2.5}$) concentration in many regions across the globe (Philip et al., 2014; Jimenez et al., 2009; Hansen et al., 2003; Brewer and Adlhoch, 2005).

The degree to which species enter the aqueous phase and participate in cloud processing is dependent upon species' intrinsic chemical properties, such as solubility and reactivity, and also upon microphysical characteristics of the droplet spectrum (Schwartz, 1986; Schwartz and Frieburg, 1981; Sander, 1999; Pandis et al., 1990; Fahey et al., 2005). The processes of droplet activation, scavenging, and chemical production lead to shifts in the aerosol size/composition distribution after droplet evaporation. These changes to the aerosol distribution then further impact aerosol transport and microphysics along with the direct and indirect radiative effects associated with that aerosol (Kreidenweis et al., 2003). The chemistry and (micro)physics of clouds and fogs must therefore be well represented in models in order to effectively assess the impacts of emissions changes on future air quality and climate.

The Community Multiscale Air Quality (CMAQ) modeling system (Byun and Schere, 2006) is a widely used state-of-the-science chemical transport model, applied on a range of scales for research, regulatory, and forecasting purposes. In the United States, it is among the most commonly used air quality models in attainment demonstrations for National Ambient Air Quality Standards for ozone and $\text{PM}_{2.5}$ (US EPA, 2007). In such frameworks, air quality simulations may be required for many emission scenarios, large domains, and/or long time periods. It is important therefore that the selected modeling system be as efficient as possible while also

being able to faithfully capture the most important chemical and physical processes affecting the pollutants of interest and their response to emission changes.

Due in part to computational constraints, historically, only a simple description of aqueous-phase chemistry has been implemented in many regional air quality models. Cloud chemistry in CMAQ (AQCHEM), for example, is based on the cloud module of the Regional Acid Deposition Model (RADM) (Walcek and Taylor, 1986) with minimal updates to the mechanism in recent years (Carlton et al., 2008). When the cloud chemistry module is called, species are distributed between gas, interstitial aerosol, and aqueous phases instantaneously depending upon the initial modal aerosol distribution and solubility. At each time step, a bisection method is used to solve for the bulk droplet pH and the associated phase/ionic distribution of model species based on known total concentrations and assuming electroneutrality and thermodynamic equilibrium. Activity coefficients, estimated with the Davies equation, are applied to ionic species in solution. A forward Euler method is used to solve a set of seven oxidation reactions, with time stepping based on the reaction rates and precursor/oxidant concentrations for sulfate production alone. The seven reactions represented are the oxidation of aqueous SO_2 by hydrogen peroxide, ozone, oxygen (catalyzed by iron and manganese), methyl hydroperoxide, and peroxyacetic acid as well as two reactions that parameterize SOA formation from glyoxal and methylglyoxal. Scavenging of interstitial aerosol and wet deposition is calculated alongside the chemical kinetics and mass transfer (Binkowski and Roselle, 2003). Because the mechanism is hard-coded into the solver, as well as the solver's potential stability issues when applied to stiff systems of ordinary differential equations (ODEs), it is difficult to expand CMAQ's current cloud chemistry treatment to additional complex chemistry for other species. It has long been understood, however, that the aqueous-phase chemistry of clouds and aerosols affects a myriad of species, and we may be insufficiently representing cloud chemistry with our simple mechanism geared mainly towards sulfur oxidation. While computational efficiency remains important, it is also crucial for models to represent important new scientific discoveries and newly understood physicochemical processes faithfully. As computational capabilities expand and field and laboratory studies continue to elucidate additional potentially important atmospheric aqueous chemistry pathways, it is increasingly important to maintain a modeling framework that allows for ready expansion to and investigation of that chemistry.

With these motivations, the Kinetic PreProcessor (KPP) version 2.2.3 (Damian et al., 2002) has been applied to generate a Rosenbrock solver for the CMAQ cloud chemistry mechanism (AQCHEM – KMT) as well as an expanded mechanism that includes additional aqueous secondary organic aerosol formation from biogenic-derived epoxides (Pye et al., 2013) in cloud (AQCHEM – KMTI). The KPP

Table 1. Comparison of cloud chemistry models included in CMAQv5.1.

Process	AQCHEM standard	AQCHEM – KMT	AQCHEM – KMTI
Solver	Forward Euler	Rodas3 (Rosenbrock)	Rodas3 (Rosenbrock)
Gas–aqueous mass transfer	Henry’s law equilibrium	Kinetic mass transfer with gas diffusion/interfacial limitation	Kinetic mass transfer with gas diffusion/interfacial limitation
Ionic dissociation	Equilibrium	Forward/reverse reactions	Forward/reverse reactions
Chemistry	5 SO ₂ to SO ₄ ²⁻ oxidation reactions + 2 SOA-forming reactions from glyoxal and methylglyoxal	Same mechanism as AQCHEM (includes aqueous diffusion correction for O ₃)	AQCHEM mechanism + IEPOX/MPAN chemistry (includes aqueous diffusion correction for O ₃ , and IEPOX/MPAN)
pH	[H ⁺] estimated at each time step using a bisection method while maintaining electroneutrality	Dynamic [H ⁺] (initial value is based on activated aerosol ions at $t = 0$ assuming electroneutrality)	Dynamic [H ⁺] (initial value is based on activated aerosol ions at $t = 0$ assuming electroneutrality)
Other	Instantaneous activation of all accumulation- and coarse-mode species	Instantaneous activation of all accumulation- and coarse-mode species	Instantaneous activation of all accumulation- and coarse-mode species

implementation includes kinetic mass transfer between the gas phase and cloud droplets, dissociation/association, chemical kinetics, interstitial aerosol scavenging, and wet deposition and is readily expandable to larger chemical mechanisms. In the following sections, the details of the development and implementation of these additional in-cloud aqueous-phase chemistry options are presented. In Sect. 2, the AQCHEM – KMT/AQCHEM – KMTI structure is detailed alongside a description of the box model testing used in choosing solver parameters and examining the direct impacts of kinetic mass transfer and alternate solvers on predicted concentrations. In Sect. 3, the impacts of the updated cloud chemistry options are examined for winter- and summer-month regional CMAQ simulations. Some of the benefits and drawbacks of these newly implemented cloud chemistry options are discussed in Sect. 4, along with some directions for future development work and applications.

2 Aqueous-phase chemistry model description and box model testing

Table 1 contrasts the main features of the three cloud chemistry options examined here. Building upon the approach outlined by Baek et al. (2011), we used the KPP version 2.2.3 to automatically generate Fortran90 code for the numerical integration of the CMAQ in-cloud aqueous-phase chemical mechanism (Damian et al., 2002; Sandu and Sander, 2006). KPP is a free software tool that translates chemical mechanism information (e.g., species, reactions, rate coefficients) into Fortran90, Fortran77, Matlab, or C code to efficiently integrate chemical kinetics. KPP includes multiple stiff numerical integrators and has a modularity that allows rapid and straightforward testing of alternative solvers and mech-

anisms. It may also be used to generate the tangent linear or adjoint models for a given system, but this capability is not investigated here. Minor changes were made to the generated code to account for our system and I/O requirements. The model driver (for 0-D box model and CMAQ implementation) was developed outside of KPP.

AQCHEM – KMT solves the processes of phase transfer, chemical kinetics, ionic dissociation/association, scavenging of interstitial aerosol, and wet deposition. Here, AQCHEM – KMT maintains the same initialization and post-cloud redistribution assumptions as in AQCHEM, including (1) at the start of cloud processing, accumulation- and coarse-mode aerosols are instantaneously activated to droplets, all N₂O₅(g) is converted to HNO₃(g), and all H₂SO₄(g) is transferred to aqueous-phase SO₄²⁻; (2) at the end of cloud processing, HNO₃(g) and accumulation-mode aerosol NO₃⁻, as well as NH₃(g) and accumulation-mode aerosol NH₄⁺, are redistributed to retain their initial (i.e., pre-cloud) gas/aerosol phase distributions; and (3) all non-volatile aqueous-phase mass production is added to the accumulation mode (Binkowski and Roselle, 2003). Initial gas and aqueous concentrations (in units of molecules cm⁻³ air) are calculated based on their initial phase distribution, temperature/pressure, and any additional simplifying assumptions that may apply (e.g., H₂SO₄ mentioned above). As in AQCHEM, the hydroxyl radical (OH) concentration is kept constant, with droplet concentrations estimated from the initial gas-phase OH using Henry’s law. Initial [H⁺] is estimated from an ion balance on the instantaneously activated ionic species, OH⁻, and completely dissolved gaseous species (i.e., H₂SO₄(g)) at $t = 0$ s. H⁺ and other gas, aqueous, and aerosol species’ concentrations then evolve dynamically for the duration of cloud processing.

After initialization, AQCHEM – KMT solves the following system of ODEs:

$$\frac{dC_{g,i}}{dt} = -k_{mt,i}w_L C_{g,i} + \frac{k_{mt,i}}{H_i RT} C_{aq,i} \quad (1)$$

$$\frac{dC_{aq,i}}{dt} = k_{mt,i}w_L C_{g,i} - \frac{k_{mt,i}}{H_i RT} C_{aq,i} + P_{aq,i} - L_{aq,i} C_{aq,i} \quad (2)$$

$$\frac{dC_{aaero,i}}{dt} = -L_{aaero,i} C_{aaero,i}, \quad (3)$$

where

- $C_{g,i}$ is the gas-phase concentration of species i (molecules cm^{-3} air).
- $C_{aq,i}$ is the aqueous-phase concentration of species i (molecules cm^{-3} air).
- $C_{aaero,i}$ is the interstitial (Aitken) aerosol concentration of species i (molecules cm^{-3} air).
- $k_{mt,i}$ is the mass transfer coefficient of species i .
- w_L is the liquid water content fraction ($\text{cm}^3 \text{H}_2\text{O} / \text{cm}^3$ air).
- H_i is the Henry's law coefficient of species i .
- R is the gas constant.
- T is the temperature (K).
- $P_{aq,i}$ is the rate of production of species i in the aqueous phase. This includes contributions from chemical reactions (R_{aq}), scavenging of interstitial aerosol (A_{scav}), and dissociation/association of ionic species ($X_{ion,f/b}$).
- $L_{aq,i}$ is the loss term for aqueous species i . This includes loss due to chemical reactions (R_{aq}), dissociation/association of ionic species ($X_{ion,f/b}$), and wet deposition (W_{dep}).
- $L_{aaero,i}$ is the loss term for interstitial (Aitken) aerosol species i due to scavenging by cloud droplets (A_{scav}).

The rate expressions for these processes are further detailed in Table 2. The first two terms in Eqs. (1) and (2) represent the concentration changes due to mass transfer between the gas and aqueous phases. While instantaneous Henry's law equilibrium is assumed for all species in AQCHEM, in actuality, the distribution of a species between the gas and aqueous phases may deviate significantly from equilibrium (Audiffren et al., 1998; Sander, 1999; Gong et al., 2011). As in Schwartz (1986), the combined impacts of gas-phase diffusion and interfacial mass transport limitations are incorporated into a single mass transfer coefficient (k_{mt}), the expression for which is given in Table 2. Table S1 lists the mass

transfer “reactions” considered here, as well as the constants used in the mass transfer coefficient calculation.

Once in the droplet, species are allowed to dissociate into ions, represented here as forward and reverse reactions, as well as participate in irreversible chemical reactions. The hydrogen ion, $[\text{H}^+]$, crucial in determining species' phase and ionic distributions and reaction rates, is allowed to evolve dynamically from its initial value. Ionization and chemical kinetic reactions and associated rate coefficients are listed in Tables S2 and S3, respectively. Concentration gradients may develop within the droplet for some species that participate in rapid aqueous-phase reactions (e.g., O_3 ; Jacob, 1986; Walcek and Taylor, 1986). In such cases, a correction factor Q may be applied to account for aqueous-phase diffusion limitations on the overall reaction rate (Table 2) (Schwartz and Freiberg, 1981). This factor is also applied to other species to maintain consistent treatment between aqueous aerosol and cloud droplet chemistry (i.e., isoprene epoxydiol/methacrylic acid epoxide chemistry; Pye et al., 2013). Box model tests indicate, however, that aqueous diffusion impacts on the evolution of the chemical system are minimal. As the chemical mechanism evolves, aqueous diffusion limitations may become more important and will be revisited. Wet deposition (of all aqueous species) and interstitial aerosol scavenging (for Aitken-mode aerosol species) are represented as first-order loss processes. Additional information on their rate coefficients can also be found in Table 2. A list of CMAQ and “local” AQCHEM – KMT(I) species is given in Table S4.

2.1 Solver selection and tolerance settings

A previous comparison of several stiff ODE solvers applied for different types of atmospheric chemical systems indicated that Rosenbrock solvers are some of the most efficient at solving computationally intensive multiphase chemistry problems for modest accuracies (Sandu et al., 1997a, b). KPP offers several Rosenbrock integrator options. In an effort to determine the optimal solver for our mechanism, we applied each KPP Rosenbrock solver with a positive definite adjustment (Sander et al., 2011) to over 20 000 scenarios (Table S5) representing a range of atmospheric conditions and then compared the results to a reference solution generated with the variable-coefficient ordinary differential equation solver (VODE). VODE is an initial-value ODE solver that uses variable-coefficient backward differentiation formula (BDF) methods for stiff systems and may be viewed as a successor to the Livermore solver for ordinary differential equations (LSODE) (Hindmarsh, 1983), which historically has been commonly applied to generate reference solutions for atmospheric chemistry problems (Brown et al., 1989; Sandu et al., 1997b). DVODE (VODE with double precision) was downloaded from the Netlib repository (<http://www.netlib.org>) and applied to the rate equations and Jacobian for the system of AQCHEM – KMT reactions to generate a reference solution as well as provide an independent check on the codes

Table 2. Modeled processes and associated rate coefficients and equations.

Process	Equations	Rate coefficients	Other information*
Gas–liquid phase transfer	$C_{g,i} \xrightarrow{k_f} C_{aq,i}$	$k_f = k_{mt,i} w_L$	$k_{mt,i} \left(s^{-1} \frac{\text{vol}_{\text{air}}}{\text{vol}_{\text{H}_2\text{O}}} \right) = \left(\frac{r^2}{3D_{g,i}} + \frac{4r}{3\bar{v}_i\alpha_i} \right)^{-1}$
Liquid–gas phase transfer	$C_{aq,i} \xrightarrow{k_b} C_{g,i}$	$k_b = \frac{k_{mt,i}}{H_{T,i}RT}$	$\bar{v}_i = \sqrt{\frac{8RT}{MW_i\pi}}$
$X_{\text{ion},f}$: Dissociation	$C_{aq,i} \xrightarrow{k_f} C_{aq,i}^{-1} + H^+$	$k_b = \text{literature value, } T \text{ independent}$	$K_{\text{eq},i,T} = K_{\text{eq},i,T_{\text{ref}}} \left[\frac{-\Delta H_a}{R} \left(\left(\frac{1}{T} \right) - \left(\frac{1}{T_{\text{ref}}} \right) \right) \right]$ Activity coefficients are rolled into the forward and backward rates as appropriate
$X_{\text{ion},b}$: Association	$C_{aq,i}^{-1} + H^+ \xrightarrow{k_b} C_{aq,i}$	$k_f = K_{\text{eq},i,T} k_b$	
A_{scav} : Droplet scavenging of interstitial aerosol	$C_{aer,i,akn} \xrightarrow{\alpha} C_{aq,i}$	α	α is the attachment rate for interstitial aerosols, calculated external to the aqueous chemistry module according to Binkowski and Roselle (2003)
W_{dep} : Wet deposition	$C_{aq,i} \xrightarrow{W_{\text{dep}}} C_{WD,i}$	$W_{\text{dep}} = \frac{1}{\tau_{\text{wash}}}$	$\tau_{\text{wash}} \text{ (s)} = \frac{WT_{\text{AVG}} \times C_{\text{THK}} \times 3600}{\text{PRATE}}, 0$ where WT_{AVG} = total liquid water content, C_{THK} = cloud thickness, PRATE = precipitation rate
R_{aq} : Chemical kinetics	$C_{aq,1} + C_{aq,2} \xrightarrow{k_{\text{rxn}}} C_{aq,3}$	k_{rxn}	Complex rate coefficients are set according to the CMAQ base mechanism (Sarwar et al., 2013; Carlton et al., 2010). While most droplet species are assumed to be well-mixed, a correction factor may be applied to account for aqueous diffusion limitations (Table S3). This correction factor, Q_i , relates surface and bulk droplet concentrations. $k_{\text{rxn,effective}} = k_{\text{rxn}} Q_i$ $Q_i = 3 \left(\frac{\coth(q_i)}{q_i} - \frac{1}{q_i^2} \right), Q_i \leq 1$ $q_i = r \sqrt{\frac{k_i}{D_{aq,i}}}$

* MW is the molecular weight; $D_{g,i}$ is the gas-phase diffusion coefficient ($\text{m}^2 \text{s}^{-1}$); α_i is the accommodation coefficient; q_i is the diffuso-reactive parameter; $D_{aq,i}$ is the aqueous-phase diffusion coefficient ($\text{m}^2 \text{s}^{-1}$); k_i is the effective first-order reaction rate of species i ; r is the droplet radius (m).

generated with KPP. The reference solution for each scenario was generated using relative and absolute tolerance settings of 10^{-8} . For a subset of the scenarios, the reference was compared with results using the fifth-order Runge–Kutta solver, RADAU5 (relative and absolute tolerances set at 10^{-8} and 10^{-4} molecules cm^{-3} , respectively). RADAU5 is a robust solver used to provide reference solutions in the previous solver intercomparison studies for atmospheric chemical systems (Sandu et al., 1997a, b). Available Rosenbrock solver versions, ROS2, ROS3, ROS4, Rodas3, and Rodas4, were applied to the test scenarios for a range of absolute and relative tolerances (absolute tolerances range from 10^{-4} to 10^4 molecules cm^{-3} air; relative tolerances range from 10^{-4} to 10^{-1}). As in Sandu et al. (1997a, b), we use significant digits of accuracy (SDAs) as a metric to describe the relative accuracy of a solver for a given tolerance set. SDA can be

defined as follows:

$$\text{SDA}_{\text{min}} = -\log_{10}(\max(\text{ER}_k)), \quad (4)$$

where k represents the CMAQ species involved in aqueous chemistry and

$$\text{ER}_k = \sqrt{\frac{1}{N} \sum \left| \frac{C_{i,k,\text{ref}} - C_{i,k}}{C_{i,k,\text{ref}}} \right|^2} \quad (5)$$

for N total i scenarios. $C_{i,k,\text{ref}}$ is the reference solution from DVODE (or RADAU5) for species k and scenario i , and $C_{i,k}$ is the concentration generated with a Rosenbrock solver for a particular tolerance set. This calculation is limited to concentrations exceeding 10^7 molecules cm^{-3} to avoid the influence of large relative errors for very small concentrations.

Figure 1a gives the SDA_{min} for each of the solver/tolerance combinations vs. the total CPU time required for all scenar-

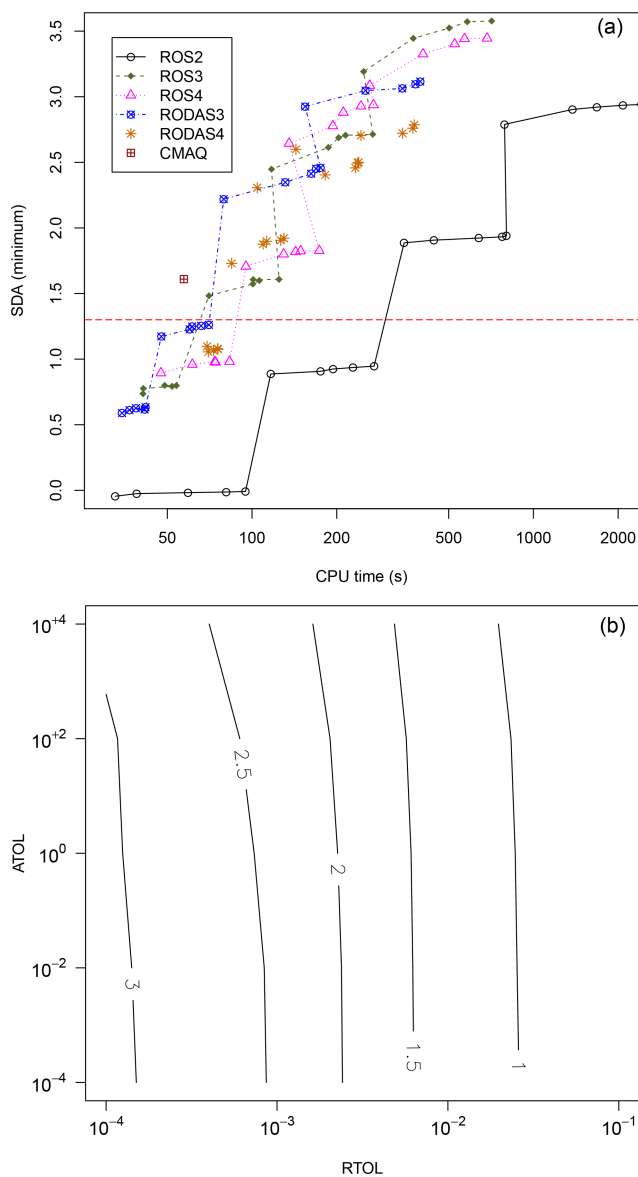


Figure 1. Significant digits of accuracy (SDAs) for the CMAQ species with the maximum error for (a) different variants of Rosenbrock solvers and (b) the Rodas3 solver at different combinations of relative and absolute tolerance. Each point in (a) represents a different relative and absolute tolerance combination. The absolute tolerances tested were 10^{-4} , 10^{-2} , 10^0 , 10^2 , and 10^4 molecules cm^{-3} air for relative tolerances of 10^{-4} , 10^{-3} , 10^{-2} , and 10^{-1} . Each “plateau” visible for certain solvers in (a) represents a different relative tolerance setting, with tighter tolerances leading to higher SDAs.

ios. This is the value for the single species that deviates furthest from the reference solution. The reference solution here is given by DVODE. Most of the Rosenbrock solvers perform similarly (ROS2 is the exception), with Rodas3 and ROS3 the most efficient at lower accuracies. If an SDA of 2 corresponds to an “accuracy” of 1 %, the dashed horizontal line in

Fig. 1a represents an accuracy of ~ 5 %. Plots here are shown only for DVODE. For the subset of scenarios tested, DVODE and RADAU5 produce results that are within 0.002 % of each other for all scenarios ($\text{SDA}_{\min} = 5.6$, with no minimum concentration setting).

Rodas3 was implemented as the default integrator in AQCHEM – KMT due to favorable performance compared to the other Rosenbrock solvers for the scenarios considered here; however, any KPP Rosenbrock solver may be invoked with a change to a single argument in the call to the integrator. Rodas3 “tolerance contours” are given in Fig. 1b. While choice of relative tolerance has a significant influence on the accuracy of the results, the solution is comparatively unaffected by the choice of absolute tolerance in the tested range, with degradation in the solution only beginning to occur at absolute tolerances exceeding 10^2 molecules cm^{-3} for the relative tolerances tested here. In an effort to be efficient while still maintaining an accuracy well within 5 % of the reference solution, we selected a default absolute tolerance of 10^2 molecules cm^{-3} air, a relative tolerance of 10^{-2} for most species, and a relative tolerance of 10^{-3} for hydrogen peroxide and glyoxal/methylglyoxal. The SDA_{\min} for this set of tolerance settings for Rodas3 is represented by the red gridded square in Fig. 1. These tolerance settings lead to ~ 2 % or better accuracy for all species for the tested scenarios, with most species well under 1 %. This selection strikes a balance between accuracy and efficiency for this mechanism. For other applications, or in the case of a chemical mechanism expansion, these values can and should be reevaluated and adjusted as necessary to maintain that balance.

2.2 Impacts of mass transfer assumptions and solver on box model predictions

While assuming instantaneous Henry’s law equilibrium to describe partitioning between gas and aqueous phases can reduce the often significant computational burden associated with simulating heterogeneous chemistry, past studies have indicated that there are species and conditions for which equilibrium conditions are not met during the lifetime of typical cloud droplets. In such cases, a kinetic mass transfer treatment may be necessary to accurately describe the phase distribution between gas and cloud or fog droplets and subsequent chemistry (Djouad et al., 2003; Audiffren et al., 1998, 1996; Chaumerliac et al., 2000; Ervens et al., 2003). Here, we treat mass transfer kinetically as a default in AQCHEM – KMT in an effort to assess how deviations from instantaneous Henry’s law equilibrium impact predicted concentrations for short- and long-term averaging periods which may be of interest in different applications.

Box model versions of AQCHEM and AQCHEM – KMT were compared for the Table S5 scenarios to better understand the potential impacts of differing solver and mass transfer treatment on aqueous-phase chemistry predictions, isolated from other processes in CMAQ that might com-

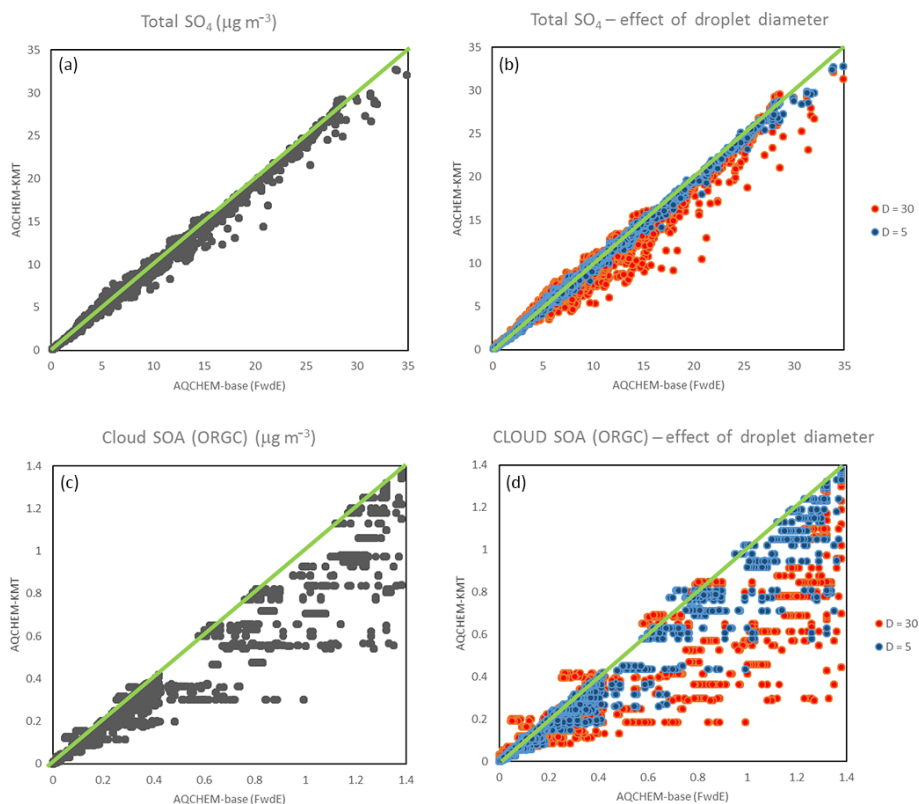


Figure 2. AQCHEM – KMT vs. standard AQCHEM predictions for (a) total SO_4^{2-} (sum over all modes) and (c) SOA from cloud processing of carbonyls (ORGC) at default droplet diameter of $16\ \mu\text{m}$ as well as at 5 and $30\ \mu\text{m}$ for (b) total SO_4^{2-} and (d) ORGC.

pligate the analysis. Here, we focus mainly on the predictions for the two species chemically produced in the standard AQCHEM mechanism, SO_4^{2-} and SOA from cloud processing of α -dicarbonyls (ORGC). Figure 2a and c show SO_4^{2-} and ORGC predictions for AQCHEM – KMT (assuming a default droplet diameter of $16\ \mu\text{m}$) vs. standard AQCHEM. For many scenarios, it appears that the equilibrium assumption is a good one, particularly for SO_4^{2-} , with many points falling along or not far from the 1:1 line. There are also significant deviations for several scenarios, especially for cloud SOA. Figure 2b and d show the impact of changing the default droplet diameter (to 5 and $30\ \mu\text{m}$) for SO_4^{2-} and ORGC, respectively. As the droplet diameter increases, deviation between AQCHEM – KMT and AQCHEM predictions for both SO_4^{2-} and ORGC increases as well. In the case of ORGC, even at small droplet diameters, there can be a large discrepancy between the models. The difference in predicted ORGC concentrations at small droplet diameters is, in part, attributable to the difference between the time-stepping technique of AQCHEM and the Rosenbrock solver in AQCHEM – KMT. AQCHEM steps forward in time based on the rate of SO_4^{2-} production and the lifetime of the cloud. These constraints can produce large time steps that can lead to higher SOA predictions. In AQCHEM – KMT, the solver

determines forward time steps based on a convergence test dependent on all species and their tolerance settings. Different predictions of ORGC also occur for larger cloud droplets when the deviation from equilibrium, due to mass transfer limitations, may become significant (Fig. S1).

Additional box modeling investigations with a slightly expanded mechanism indicate that when one ignores aqueous diffusion limitations (for the default droplet diameter of $16\ \mu\text{m}$), assumes instantaneous equilibrium for ionic dissociation, and calculates pH assuming electroneutrality (but maintains the kinetic mass transfer treatment for transfer between the phases), the predicted concentrations of SO_4^{2-} , ORGC, and other major species are comparable to those predicted with the fully dynamic approach of AQCHEM – KMT. This indicates that the largest differences between AQCHEM – KMT and AQCHEM for the test scenarios are a result of using kinetic mass transfer coefficients to describe the transfer of species between the phases (i.e., not assuming instantaneous Henry's law equilibrium) and to a lesser extent the change in solvers.

The differences in predicted SO_4^{2-} and ORGC with different droplet size (Figs. 2 and S1) and SO_4^{2-} with different values for initial pH (Fig. S2) (which represents the impact of the activated aerosol fraction) point to the potential

importance of microphysical parameters on predicted concentrations and supports the development of better linkages between aqueous chemistry and cloud microphysics codes. Other species typically show smaller differences for different droplet sizes/pH differences, but that may change with the addition of new chemistry.

It should be noted that, by introducing the new solver and relaxing equilibrium assumptions, the computational requirements of AQCHEM – KMT significantly exceed those of AQCHEM, even before adding new chemical species or reactions. On average, AQCHEM can simulate the scenarios of Table S5 with a runtime on the order of ~ 1 s, while AQCHEM – KMT requires ~ 65 s to model the scenario set. While cloud chemistry only accounts for a fraction of the computational time required by a three-dimensional chemical transport model like CMAQ, implementation of AQCHEM – KMT in a chemical transport model (CTM) will lead to an overall increase in CTM runtime that will vary depending, in part, on the cloudiness of a modeled period. These requirements will likely increase as the chemical mechanism expands, and future efforts should be dedicated to investigating how to make the model more efficient, including revisiting equilibrium assumptions for certain processes or species.

2.3 Aqueous SOA from biogenic epoxides

Using KPP to generate the code for the updated cloud chemistry module allows for straightforward extension to additional aqueous chemistry. Here, we investigated the expansion of the cloud chemistry mechanism to include the in-cloud formation of SOA from biogenic epoxides (AQCHEM – KMTI). The process is based on reactions in aerosol water incorporated into CMAQv5.1 (Pye et al., 2013). While acid-catalyzed aqueous SOA formation from species like isoprene epoxydiols (IEPOX) is expected to be more important in highly concentrated aerosol water than comparatively dilute cloud droplets (where oxidation of soluble organic compounds by the hydroxyl radical is expected to be the dominant contributor to SOA mass), some SOA may still be formed in cloud droplets from IEPOX (McNeill, 2015; Fig. 2). Overall, the aqueous-phase reaction mechanism in aerosol and cloud water is expected to be similar, but dominant reaction pathways may change between concentrated and dilute conditions (McNeill, 2015). We include these reactions here to improve consistency between CMAQ's cloud and aerosol aqueous chemistry mechanisms and to quantify the potential impacts of adding these cloud water reactions. The additional species and reactions are given in the shaded sections of Tables S1, S3, and S4 in the Supplement.

3 CMAQ simulations and measurements

The impacts of the updated solver and kinetic mass transfer treatment of AQCHEM – KMT and the additional aqueous chemistry of AQCHEM – KMTI were investigated using multiple CMAQ simulations. Simulation periods and domains were selected based on the availability of model inputs and/or specialized observations for comparison. Winter and summer periods were run to illustrate any seasonal differences in sensitivity to the different cloud chemistry modules. Simulations were conducted for winter and summer 2011 over the contiguous US (CONUS) with inputs developed to evaluate CMAQv5.1 (Appel et al., 2016), as well as for a summer period over the eastern United States coinciding with a 2013 measurement campaign that focused on SOA formation. The CONUS simulations were used to assess the impacts of kinetic mass transfer and solver (AQCHEM vs. AQCHEM – KMT), while the summer simulation over the eastern US was geared towards investigating the impact of additional in-cloud SOA formation from biogenic epoxides (AQCHEM – KMT vs. AQCHEM – KMTI). These CMAQ simulations are further detailed below. Note that in all CMAQ cases, cloud chemistry and gas-phase chemistry are not solved simultaneously but are instead solved in separate operators. Following advection and diffusion, cloud processes (including cloud chemistry) are treated for resolved and subgrid clouds. This is followed by gas-phase chemistry (including heterogeneous chemistry on aerosols) and aerosol dynamics. Inevitably there are errors that can result from estimating the impacts of chemistry of different phases separately, and in the future, the feasibility of simultaneously solving chemistry across all phases will be investigated.

Test 1: CMAQv5.1 was applied with both standard AQCHEM and AQCHEM – KMT cloud chemistry for January and July 2011 over CONUS at 12 km horizontal resolution and 35 vertical layers extending up to 50 mb. Meteorological fields were generated with the Weather Research and Forecasting (WRF) model (Skamarock et al., 2008), version 3.7, and emissions were based on the 2011 National Emissions Inventory (NEI), version 2 (<https://www.epa.gov/air-emissions-inventories/2011-national-emissions-inventory-nei-documentation>). Aerosol treatment and gas-phase chemistry were described by the AERO6 aerosol module and CB05e51 carbon bond chemical mechanism, respectively (http://www.airqualitymodeling.org/index.php/CMAQ_v5.1_CB05_updates). Additional simulation configuration options included in-line biogenic emissions, in-line plume rise, windblown dust, lightning NO_x emissions, bidirectional ammonia exchange, and in-line calculation of photolysis rates including absorption and scattering from predicted gas and aerosol concentrations. More detailed information about these CMAQ options can be found in the CMAQ

operational guidance and technical documentation available at www.cmascenter.org. Results are examined after 10 days of spinup from clean default initial conditions. Hourly lateral boundary conditions were taken from a global GEOS-Chem simulation from the same period (Henderson et al., 2014).

Test 2: The impact of adding cloud water SOA formation from IEPOX and methacryloylperoxynitrate (MPAN) products, methacrylic acid epoxide (MAE) and hydroxymethyl-methyl- α -lactone (HMML), was examined for a summer period coinciding with the Southern Oxidant and Aerosol Study (SOAS) (<http://soas2013.rutgers.edu/>). Two simulations were performed with AQCHEM – KMT and AQCHEM – KMTI for 1 June–15 July 2013, with 11 days of spinup. The base model was CMAQv5.0.2+, an interim version of CMAQ between the 5.0.2 and 5.1 official releases. Gas-phase and aerosol chemistry was simulated with the SAPRC07TIC chemical mechanism (Xie et al., 2013; Lin et al., 2013) and AERO6i aerosol module, respectively (http://www.airqualitymodeling.org/index.php/CMAQ_v5.1_SAPRC07tic_AE6i). The model was applied at a 12 km horizontal resolution over the eastern US with 35 vertical layers up to 100 mb. Emissions were generated using the 2011 NEI with the electric-generating unit (EGU) continuous emission monitoring system (CEMS) data for 2013 and an offline application of the Biogenic Emission Inventory System (BEIS) version 3.6.1 with Biogenic Emissions Land Use Database (BELD4) land cover and vegetation. Wildfire and prescribed fire emissions are based on the Satellite Mapping Automated Reanalysis Tool for Fire Incident Reconciliation (SMARTFIRE) system (<http://www.airfire.org/smartfire/>) using 2013 day-specific satellite detection of fires. Windblown dust and lightning NO_x emissions were not included, nor was bidirectional ammonia surface exchange. Meteorological inputs were generated with WRFv3.6.1. Lateral boundary conditions and initial conditions were taken from a 36 km resolution CMAQ simulation performed over CONUS, southern Canada, and northern Mexico for the same period. The boundary conditions for that coarser-resolution CMAQ simulation were derived from a GEOS-Chem simulation performed at 2° × 2.5° lateral resolution. Additional details on the modeling platform can be found in Pye et al. (2015). Simulated concentrations for 2-methyltetrols and 2-methylglyceric acid (2-MG) (i.e., two SOA products from IEPOX and MAE/HMML) were compared to measurements collected at a site in Research Triangle Park (RTP), NC, 1 June through 15 July 2013. The observed 2-methyltetrol and 2-MG concentrations were obtained via gas chromatography–mass spectrometry (GC-MS) analysis of aerosol mass from daily filter measurements using a similar methodology to that

described in Lewandowski et al. (2013), Kleindienst et al. (2010), and Edney et al. (2005).

3.1 Impact of kinetic mass transfer and Rodas3 solver

Figures 3 and 4 show the average baseline (AQCHEM) concentrations and difference in predictions between AQCHEM (base) and AQCHEM – KMT ([KMT] – [Base]) for fine SO₄²⁻ and ORGC, respectively. In addition to a map of the average baseline concentrations (panels a, d), the figures include a map of monthly average (panels b, e) and maximum hourly (panels c, f) differences for January (top) and July (bottom) 2011. In both winter and summer months, the monthly average difference in SO₄²⁻ concentration is low and does not exceed 0.2 μg m⁻³ for the model periods investigated here. Any impacts of kinetic mass transfer or solver changes on predicted SO₄²⁻ concentrations for our standard (and relatively simple) cloud chemistry mechanism are diluted when moving from aqueous chemistry box modeling to a regional modeling framework where species are impacted by additional processes and averaging periods are longer. Similarly, there are minimal differences in the winter and summer average ORGC concentrations as well. Hourly concentrations can show more significant differences for both species, however, with hourly concentration differences as high as 14.7 μg m⁻³ for SO₄²⁻ and 0.4 μg m⁻³ for ORGC. Similar to clouds themselves, these impacts are rather spatially and temporally variable. To illustrate the potential short-term differences between the base and “KMT” aqueous chemistry modules, Fig. 5a and b show the time series of the SO₄²⁻ concentration differences at the grid cell with the highest hourly concentration difference for all hours of the January (cell (264,54)) and July (cell (183, 213)) 2011 simulations, respectively. The figures also include modeled total liquid water content values. While monthly average SO₄²⁻ predicted with AQCHEM – KMT is only 5.2 and 6.5 % lower than the base in the cell selected for January and July, respectively, when the maximum hourly difference is observed, AQCHEM – KMT predicts 35 % less SO₄²⁻ at cell (264,54) and 15 % less SO₄²⁻ at cell (183,213) compared to AQCHEM. For most hours, the SO₄²⁻ concentrations are very similar for the two runs. However, when the liquid water content values become significant and the cloud chemistry module is called, the hourly differences between predicted SO₄²⁻ concentrations often exceed 2 μg per cubic meter in magnitude, with kinetic mass transfer leading nearly always here to lower predicted SO₄²⁻ concentrations due to the incorporation of gas and interfacial mass transfer limitations. During the rare times when AQCHEM – KMT predicted higher SO₄²⁻ than the base in these cells, the hourly increase in SO₄²⁻ was less than 0.26 μg m⁻³. It should be noted that since CMAQ already tends to have a slightly low bias with respect to SO₄²⁻ concentrations in the winter and summer for most regions in the US (Appel et al., 2016), without

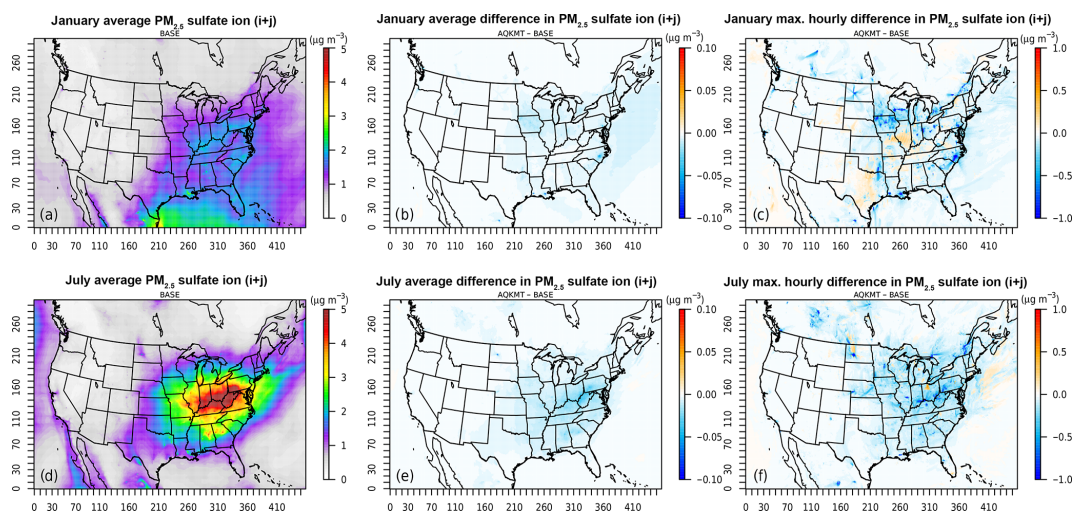


Figure 3. Average baseline (a, d) and average (b, e) and maximum (c, f) hourly difference (AQKMT – Base) in fine SO_4^{2-} ($\mu\text{g m}^{-3}$) for January and July 2011 using CMAQv5.1. Note the different scales for average baseline concentration, average difference, and maximum difference plots.

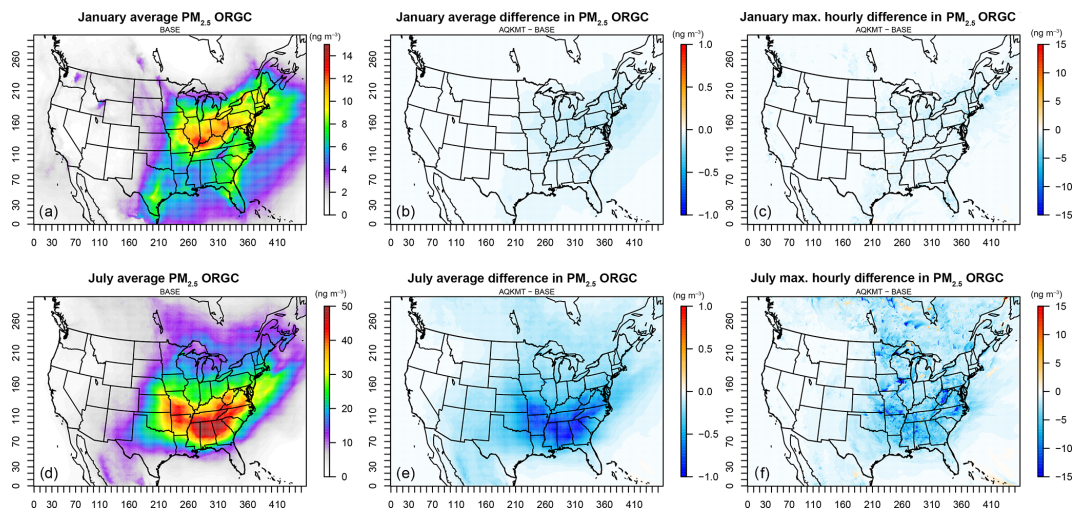


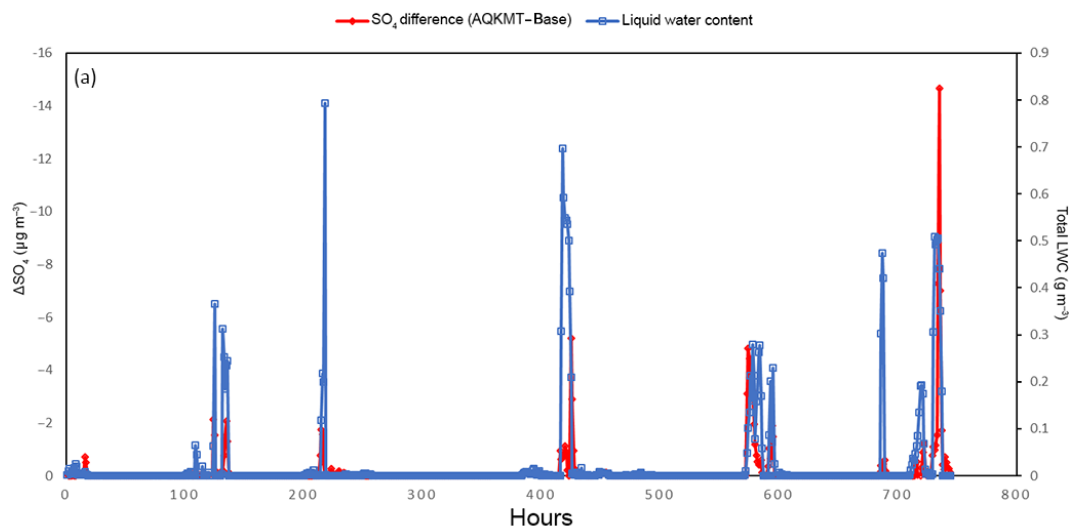
Figure 4. Average baseline (a, d) and average (b, e) and maximum (c, f) hourly difference (AQKMT – Base) in SOA from cloud processing of carbonyls (ng m^{-3}) for January and July 2011 using CMAQv5.1

additional updates to chemistry or improved cloud parameter predictions, AQCHEM – KMT will lead to a small increase in absolute bias for SO_4^{2-} at most surface sites in our domain compared to AQCHEM.

Absolute ORGC mass predictions are less impacted than SO_4^{2-} , but these tend to be low on average in the base case and may have limited sensitivity to changes in mass transfer treatment due in part to CMAQ's implementation of cloud SOA formation. In AQCHEM – KMT (as in AQCHEM), ORGC is formed from the reaction of glyoxal and/or methylglyoxal with the hydroxyl radical. The hydroxyl radical concentration is estimated at the start of cloud processing based on the initial gas-phase concentration (Henry's law) and held constant for the duration of the "master" cloud time step (i.e.,

mass transfer limitations are not considered for OH). This was done in part to compensate for the lack of a more complete treatment of radical/organic chemistry in the aqueous phase, along with a relatively loose coupling between gas and aqueous chemistry in CMAQ. A constant oxidant concentration may cause an artificially high rate of consumption of the precursor species and insensitivity of the reaction to droplet size and associated mass transfer limitations. In fact, it has been suggested that in-cloud oxidation of organic species by OH may be oxidant limited due in part to the effects of mass transfer limitations on aqueous OH concentrations (Ervens et al., 2014). If a more explicit cloud SOA mechanism was included where OH concentrations were allowed to vary, mass

Time series of LWC and ΔSO_4 IJ (AQKMT– Base) at cell with max hourly difference at the surface for January 2011 (264,54)



Time series of LWC and ΔSO_4 IJ (AQKMT– Base) at cell with max hourly difference at the surface for July 2011 (183,213)

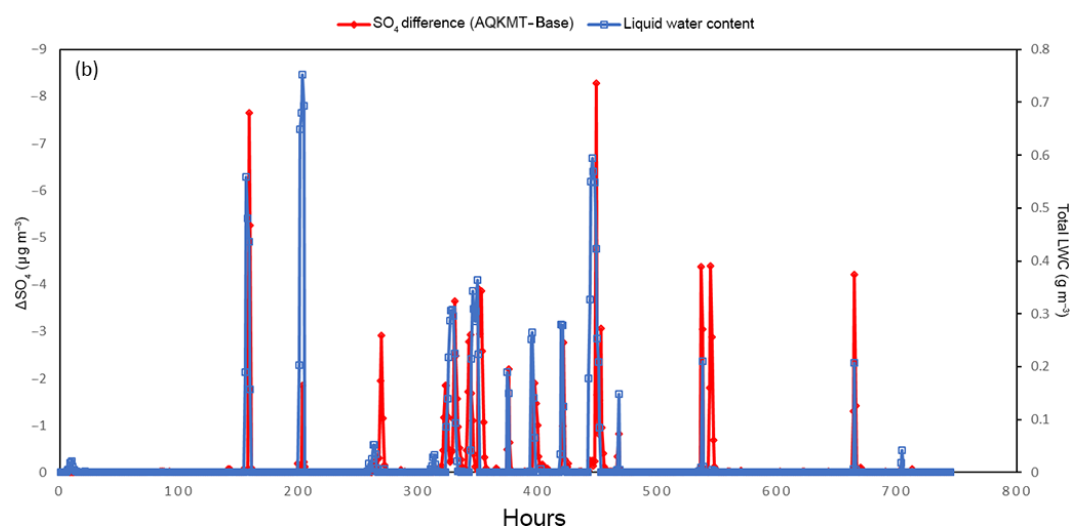


Figure 5. Modeled hourly liquid water content (blue, g m^{-3}) and change in fine SO_4^{2-} (red, $\mu\text{g m}^{-3}$) (AQKMT – Base) in the cell containing the maximum (absolute) hourly difference for (a) January and (b) July 2011.

transfer limitations would likely have a greater influence on in-cloud SOA production.

3.2 Impact of cloud SOA formation pathway from biogenic epoxides

More than half of fine particulate mass ($\text{PM}_{2.5}$) can be made up of organic compounds, with a significant secondary fraction, depending on location and season. While it is an inherently difficult system to fully characterize due to the number of compounds involved, progress has been made in identifying precursor compounds and important pathways lead-

ing to SOA formation. Recently, SOA formation from isoprene epoxydiols (IEPOX) and MPAN products via reactive uptake to aerosol water was implemented in CMAQ (Pye et al., 2013). The aqueous chemical mechanism does not necessarily differ between aerosol and cloud water, but certain reactions may be more important in the different regimes (i.e., concentrated vs. dilute) (McNeill, 2015; Herrmann et al., 2015). Here, we explore the impacts of including the aqueous IEPOX/MPAN SOA reaction pathway in cloud water and apply the model to an eastern US domain coinciding with SOAS. The platform/period is well suited for the task due to the availability of frequent 2-methyltetrol and 2-MG

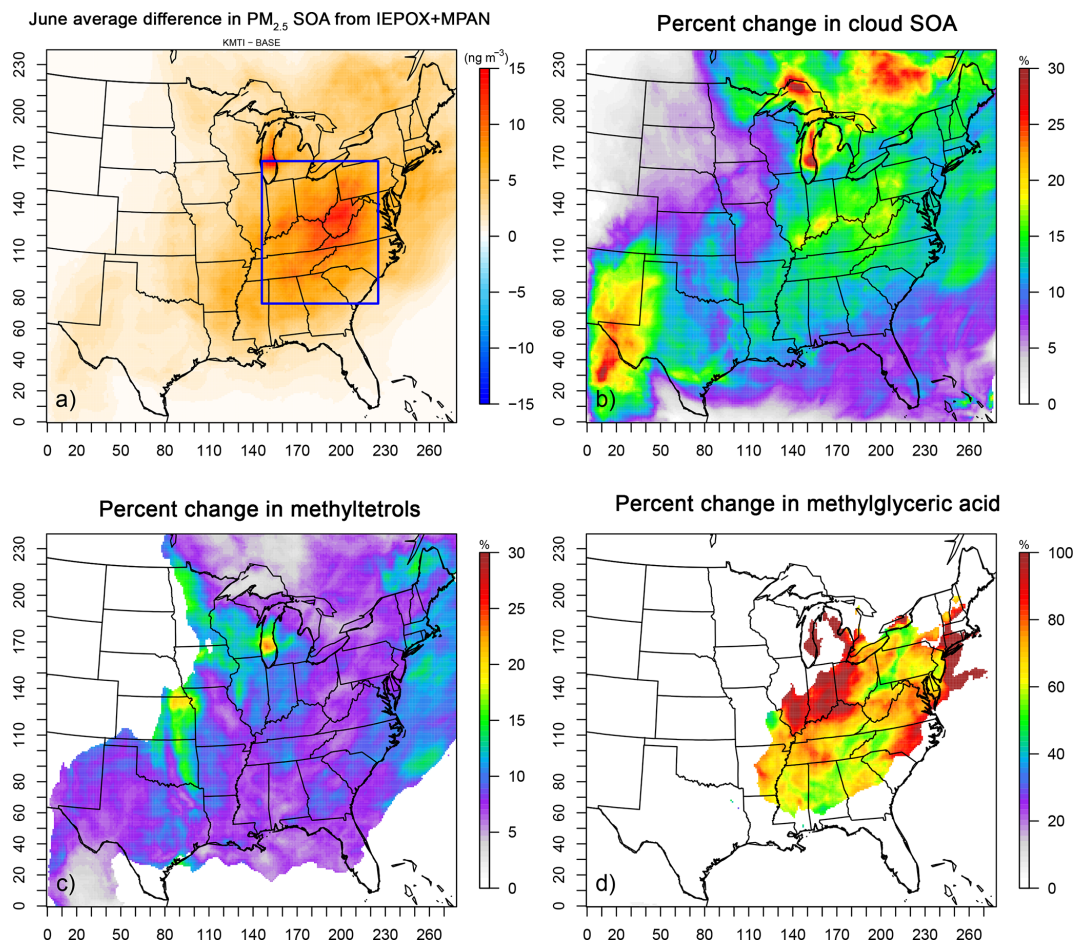


Figure 6. (a) June 2013 average increase in SOA from IEPOX/MPAN and percentage increase in surface-level (b) “cloud SOA” ($> 1 \text{ ng m}^{-3}$), (c) 2-methyltetrols ($> 10 \text{ ng m}^{-3}$), and (d) 2-MG ($> 1 \text{ ng m}^{-3}$). “SOA from IEPOX + MPAN” is the sum of 2-methyltetrols, 2-MG, and related organosulfates, organonitrates, and oligomers.

measurements, products of the aforementioned reaction pathways (Table S3), at multiple sites.

Figure 6 shows the modeled June 2013 average SOA increases due to including IEPOX/MPAN chemistry in cloud droplets. Each panel gives an absolute or percentage concentration difference of impacted SOA species between the extended chemistry (AQCHEM – KMTI) and standard chemistry (AQCHEM – KMT) simulations. In the areas of highest baseline concentrations of IEPOX/MPAN SOA, cloud chemistry contributes an additional ~ 5 – 13% to the June average concentration, with a maximum increase in average IEPOX/MPAN SOA of $\sim 20 \text{ ng m}^{-3}$ (Fig. 6a). Total SOA from IEPOX/MPAN here is a sum of 2-methyltetrols, 2-MG, organosulfates, organonitrates, and dimers. There is a more significant relative impact (i.e., percentage increase as opposed to absolute mass change) on 2-MG (Fig. 6d) than 2-methyltetrols (Fig. 6c). Note, however, that 2-MG concentrations are an order of magnitude lower than those of methyltetrols. The impact on organosulfate (OS), organonitrate (ON), and dimer concentrations with the additional

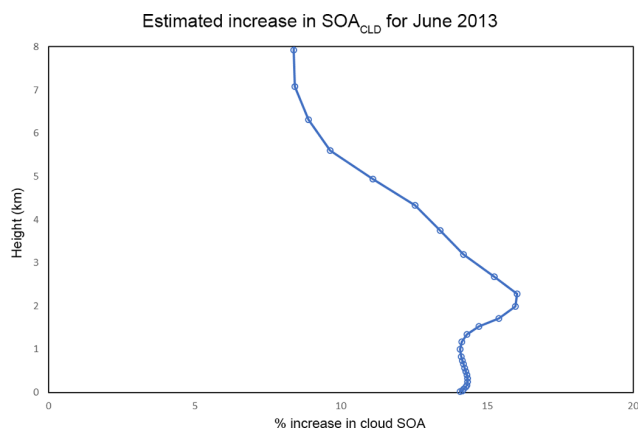


Figure 7. June 2013 average vertical distribution of the estimated percentage increase in cloud SOA with the addition of SOA from IEPOX/MPAN in cloud water. These values are averaged spatially over the area indicated by the blue box in Fig. 6a.

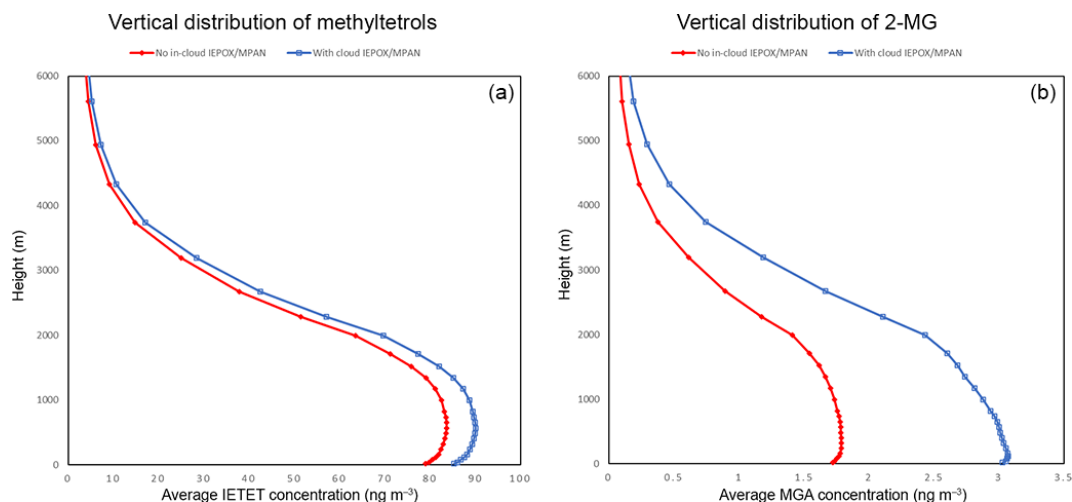


Figure 8. June 2013 vertical distribution of (a) 2-methyltetrols (ng m^{-3}) and (b) 2-MG (ng m^{-3}), averaged spatially over the area indicated by the blue box in Fig. 6a.

cloud chemistry is negligible, supporting previous work suggesting that OS formation would be minimal at the dilute conditions characteristic of cloud droplets (McNeill et al., 2012). The additional cloud SOA chemistry leads to an average increase of $\sim 10\text{--}20\%$ in surface-level cloud SOA (i.e., SOA formed within CMAQ cloud water) in the eastern US (Fig. 6b). The largest relative increases in cloud SOA occur, as expected, in areas with periods of persistent cloud cover and high liquid water content during the modeling period (e.g., Lake Michigan).

For the area inside the blue rectangle in Fig. 6a, the average vertical concentration differences due to the additional IEPOX/MPAN cloud chemistry are shown in Figs. 7 and 8. There is a 14–16% increase in average cloud SOA concentrations from the surface to 3 km, with a peak percentage increase just above 2 km. This translates to a spatially/temporally averaged IEPOX/MPAN SOA concentration increase of 8 ng m^{-3} in the layers closest to the surface (Fig. 8). Larger impacts can be seen during shorter timescales at locations that are characterized by the availability of both adequate precursor levels and cloud liquid water content (Fig. 11).

PM filters were analyzed for the tracer compounds, 2-methyltetrols and 2-MG, at select sites during the SOAS field campaign (Budisulistiorini et al., 2015). A comparison of modeled and measured concentrations of these species at the RTP site in NC (where some of the largest modeled differences occur of the available measurement sites) are given in Fig. 9. While the impacts of the additional cloud chemistry at RTP during this period are not very large, there are small increases in 2-methyltetrol and 2-MG predictions. This leads to slightly better error statistics due to the fact that the base model tends to underpredict the concentrations of these compounds at the RTP site (Table 3). While the ad-

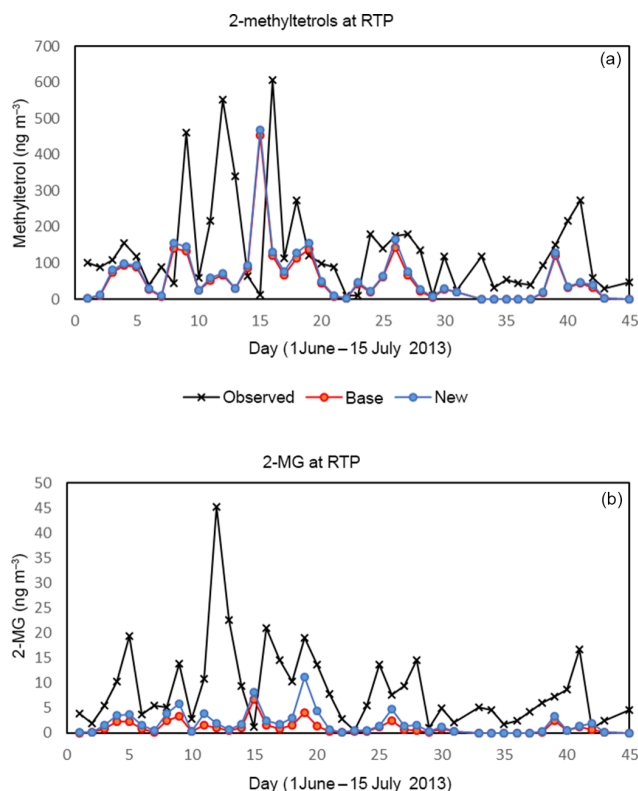


Figure 9. Observed and modeled (a) 2-methyltetrols (ng m^{-3}) and (b) 2-MG (ng m^{-3}) at Research Triangle Park (RTP), NC, during 1 June–15 July 2013, for a base (red) simulation and a simulation with additional in-cloud formation of IEPOX/MPAN SOA (blue).

ditional cloud chemistry does not drastically increase concentrations at RTP, there are areas where modeled concentration impacts can be significant (Fig. 10). To investigate under what conditions the largest contributions from cloud

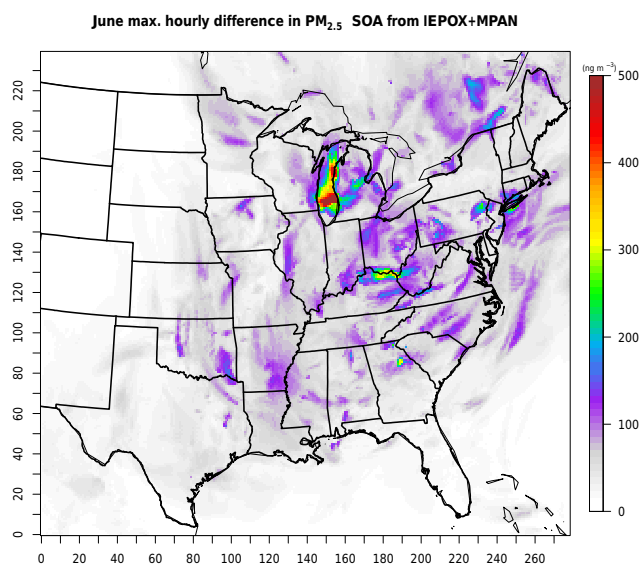


Figure 10. Maximum increase in hourly IEPOX/MPAN SOA ($[AQCHEM - KMTI] - [AQCHEM - KMT]$) (ng m^{-3}) for June 2013.

Table 3. Observation–prediction statistics for 2-methyltetrols and 2-MG at the RTP measurement site during SOAS.

	2-MG		2-methyltetrols	
	Base	New	Base	New
Normalized mean bias	−88.2	−78.6	−58.6	−54.8
Normalized mean error	91.1	83.0	79.2	77.5
Correlation	0.21	0.29	0.16	0.17
Model avg. (ng m^{-3})	1.03	1.86	56.8	61.9

water production of IEPOX/MPAN SOA might be observed, we extracted the time series of products and precursors at the cell with the largest hourly impact during the June 2013 simulation in Fig. 11. Figure 11 shows the hourly change in total SOA from the IEPOX/MPAN pathways ($\Delta\text{SOA}_{\text{IEPOX/MPAN}}$), change in 2-MG ($\Delta\text{SOA}_{2\text{-MG}}$), liquid water content, and precursor species IEPOX and MAE for the maximum difference cell. The additional chemistry included here does not lead to a temporally uniform change in concentrations, with impacts from additional cloud SOA only discernible for sporadic spikes during the latter part of the month. The large SOA impacts coincide with periods of simultaneously high liquid water content and high precursor concentrations. A large fraction of the total increase in $\text{SOA}_{\text{IEPOX/MPAN}}$ (red line) is due to increases in 2-MG production (grey line) even though 2-methyltetrols dominate the concentration of total $\text{SOA}_{\text{IEPOX/MPAN}}$ in most of the domain. If the Henry's law coefficient for IEPOX is much higher than used here (for example, 1.7×10^8 ; Gaston et al., 2014), then aqueous processing of IEPOX would lead to even higher methyltetrol concentrations than predicted here.

One of the more uncertain aspects of this chemistry may be the production of SOA from the MPAN products. In the current model formulation, 2-MG production is mainly based on the physical constants/chemical reaction rates for MAE. However, other studies have indicated that HMML may be a more dominant precursor to 2-MG (Nguyen et al., 2015). Additionally, we assume that the products of these aerosol and cloud aqueous pathways are nonvolatile, while monomeric species like 2-methyltetrols and 2-MG may be better represented as semivolatile (Isaacman-Van Wertz et al., 2016). These are areas that may be worthwhile to further refine in future development efforts, as more laboratory/field research becomes available, in an effort to better quantify the relative impacts of cloud vs. aerosol water production pathways on SOA mass.

4 Summary and future directions

We have developed a framework for extending CMAQ cloud chemistry and have implemented two additional cloud chemistry options, AQCHEM – KMT and AQCHEM – KMTI, in CMAQv5.1. While CMAQ's standard cloud chemistry module (AQCHEM) is structurally limited to a simple chemical mechanism, this work advances our ability to implement and investigate additional aqueous chemical pathways and the impacts of microphysical parameters on cloud chemistry in CMAQ.

KPP was used to generate a Rosenbrock solver to integrate the stiff system of ODEs that describe the mass transfer, chemical kinetics, and scavenging processes of CMAQ clouds. Box model tests were performed to choose efficient solver and tolerance settings, validate the code generated with KPP, and examine the potential impacts of the new solver and mass transfer limitations on model concentrations of SO_4^{2-} and SOA. Month-long winter and summer CMAQ simulations over CONUS reveal that while the new solver and mass transfer considerations do not cause large changes in regional or long-term average concentrations for the standard aqueous mechanism, more significant impacts are observed on shorter timescales. The addition of in-cloud SOA production from IEPOX/MPAN species led to an average increase in cloud SOA concentrations of around 15% for June 2013 and slightly improved error and bias statistics for IEPOX/MPAN SOA at the RTP measurement site during the SOAS field campaign period.

While the new solver and kinetic mass transfer treatment produced sporadic and small differences on average for the standard cloud chemistry mechanism, a significant value in AQCHEM – KMT is that, with the automatic code generation of KPP, the modeling framework provides a straightforward way to implement and test new chemical pathways and determine the sensitivity of model concentrations to uncertain parameters and representations. Including kinetic mass transfer treatment allows cloud chemistry, wet deposition,

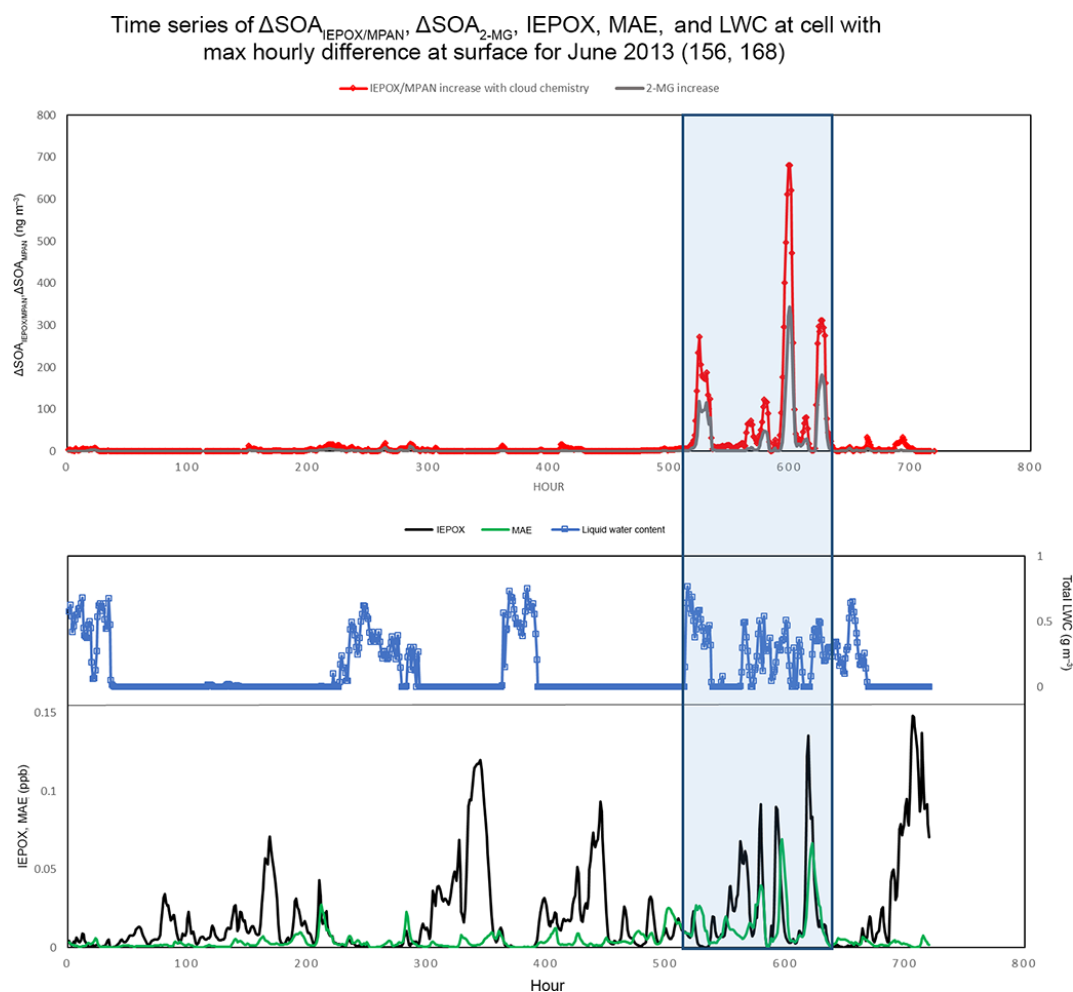


Figure 11. Change in $\text{SOA}_{\text{IEPOX/MPAN}}$ due to in-cloud production (alongside precursor and liquid water content levels) for the cell containing the highest hourly difference during June 2013. Shown from top to bottom are (top) the change in predicted hourly concentrations of total $\text{SOA}_{\text{IEPOX/MPAN}}$ (ng m^{-3}) (red) and 2-MG (ng m^{-3}) (grey) with the additional in-cloud SOA production, (middle) cell liquid water content (g m^{-3}) (blue), and (bottom) IEPOX (ppb) (black) and MAE (ppb) (green) concentrations. Between 500 and 650 h, on average, more than 40 % of the additional SOA was 2-MG.

and the distribution of species between phases to be more directly affected by microphysical parameters like droplet size. Adding linkages between cloud chemistry and microphysical parameters (e.g., cloud droplet radius or activated aerosol fraction) allows for a better representation of feedback between clouds, aerosols, and radiation, increasing our ability to determine what linkages are most influential on the model species or processes of greatest interest.

While incremental improvements in the computational efficiency occurred throughout the development process of AQCHEM – KMT, it can contribute to longer CMAQ runtimes compared to AQCHEM (6–35 % for the scenarios investigated here). Chemical transport models like CMAQ require a balance between accuracy and efficiency, and that balance often depends on the goal of a particular model application. For applications geared towards estimating $\text{PM}_{2.5}$ over monthly or seasonal averaging times, for example, equilib-

rium assumptions likely will not lead to significant errors for the standard AQCHEM mechanism. If the focus is on individual aerosol species over shorter timescales or currently unrepresented or parameterized chemistry, however, those assumptions in AQCHEM might lead to an undesired loss in accuracy, and AQCHEM – KMT might be the preferred choice. Future implementations of extended cloud chemistry in CMAQ should continue to strive towards greater computational efficiency. Alongside efforts to expand the cloud chemical mechanism to include the most relevant/impactful chemical pathways, special efforts should also be made to improve the module efficiency, including the application of simplifying equilibrium assumptions for individual species or conditions as appropriate.

Code availability. CMAQv5.1 source code, including AQCHEM, AQCHEM-KMT, and AQCHEM-KMTI cloud chemistry options, is available via a Github repository at <https://github.com/usepa/cmaq>. KPPv2.2.3 can be downloaded from the Kinetic PreProcessor website at the following location: <http://people.cs.vt.edu/asandu/Software/Kpp/>. SOAS field data are available at <http://esrl.noaa.gov/csd/groups/csd7/measurements/2013senex/>. Model data are available upon request.

The Supplement related to this article is available online at doi:10.5194/gmd-10-1587-2017-supplement.

Competing interests. The authors declare that they have no conflict of interest.

Disclaimer. Although this paper has been subjected to US EPA review and approved for publication, the views and interpretations in this publication are those of the authors and not necessarily reflective of their organizations' policies or views.

Acknowledgements. We would like to thank Jon Pleim, Deborah Luecken, and Shawn Roselle for constructive comments on our manuscript, as well as Rohit Mathur, Neha Sareen, Jason Surratt, and Barbara Turpin for helpful discussion during the course of this work. The contributions of Charles Stanier and Jaemeen Baek were supported, in part, by grant RD-83386501-0 from the Environmental Protection Agency.

Edited by: M. Long

Reviewed by: three anonymous referees

References

- Appel, K. W., Napelenok, S. L., Foley, K. M., Pye, H. O. T., Hogrefe, C., Luecken, D. J., Bash, J. O., Roselle, S. J., Pleim, J. E., Foroutan, H., Hutzell, W. T., Pouliot, G. A., Sarwar, G., Fahey, K. M., Gantt, B., Gilliam, R. C., Kang, D., Mathur, R., Schwede, D. B., Spero, T. L., Wong, D. C., and Young, J. O.: Overview and evaluation of the Community Multiscale Air Quality (CMAQ) model version 5.1, *Geosci. Model Dev. Discuss.*, doi:10.5194/gmd-2016-226, in review, 2016.
- Audiffren, N., Chaumerliac, N., and Renard, M.: Effects of a poly-disperse cloud on tropospheric chemistry, *J. Geophys. Res.*, 101, 25949–25965, doi:10.1029/96JD01548, 1996.
- Audiffren, N., Renard, M., Buisson, E., and Chaumerliac, N.: Deviations from the Henry's law equilibrium approach of the mass transfer between phases and its specific numerical effects, *Atmos. Res.*, 49, 139–161, doi:10.1016/S0169-8095(98)00072-6, 1998.
- Baek, J., Saide, P., Carmichael, G. R., Carlton, A. G., Carlson, J., and Stanier, C. O.: Developing Forward and Adjoint Aqueous Chemistry Module for CMAQ with Kinetic PreProcessor, 10th Annual CMAS Conference, Chapel Hill, NC, 24–26 October, 2011.
- Barth, M. C., Stuart, A. L., and Skamarock, W. C.: Numerical simulations of the July 10, 1996, stratospheric-tropospheric experiment: radiation, aerosols, and ozone (STERAO)-deep convection experiment storm: redistribution of soluble tracers, *J. Geophys. Res.*, 106, 12381–12400, doi:10.1029/2001JD900139, 2001.
- Binkowski, F. S. and Roselle, S. J.: Models-3 Community Multiscale Air Quality (CMAQ) model aerosol component, 1. Model description, *J. Geophys. Res.*, 108, 4183, doi:10.1029/2001JD001409, 2003.
- Brewer, P. F. and Adlhoj, J. P.: Trends in speciated fine particulate matter and visibility across monitoring networks in the south-eastern United States, *J. Air Waste Manage.*, 55, 1663–1674, doi:10.1080/10473289.2005.10464755, 2005.
- Brown, P. N., Byrne, G. D., and Hindmarsh, A. C.: VODE: a variable-coefficient ODE solver, *SIAM J. Sci. Stat. Comp.*, 10, 1038–1051, doi:10.1137/0910062, 1989.
- Budisulistiorini, S. H., Li, X., Bairai, S. T., Renfro, J., Liu, Y., Liu, Y. J., McKinney, K. A., Martin, S. T., McNeill, V. F., Pye, H. O. T., Nenes, A., Neff, M. E., Stone, E. A., Mueller, S., Knote, C., Shaw, S. L., Zhang, Z., Gold, A., and Surratt, J. D.: Examining the effects of anthropogenic emissions on isoprene-derived secondary organic aerosol formation during the 2013 Southern Oxidant and Aerosol Study (SOAS) at the Look Rock, Tennessee ground site, *Atmos. Chem. Phys.*, 15, 8871–8888, doi:10.5194/acp-15-8871-2015, 2015.
- Byun, D. and Schere, K. L.: Review of the Governing Equations, Computational Algorithms, and Other Components of the Models-3 Community Multiscale Air Quality (CMAQ) Modeling System, *Appl. Mech. Rev.*, 59, 51–77, 2006.
- Carlton, A. G., Turpin, B. J., Altieri, K. E., Seitzinger, S. P., Mathur, R., Roselle, S. J., and Weber, R. J.: CMAQ model performance enhanced when in-cloud secondary organic aerosol is included: comparisons of organic carbon predictions with measurements, *Environ. Sci. Technol.* 42, 8798–8802, doi:10.1021/es801192n, 2008.
- Carlton, A. G., Bhave, P. V., Napelenok, S. L., Edney, E. O., Sarwar, G., Pinder, R. W., Pouliot, G. A., and Houyoux, M.: Model representation of secondary organic aerosol in CMAQv4.7, *Environ. Sci. Technol.*, 44, 8553–8560, doi:10.1021/es100636q, 2010.
- Chang, J. S., Brost, R. A., Isaksen, S. A., Madronich, S., Middleton, P., Stockwell, W. R., and Walcek, C. J.: A three-dimensional Eulerian acid deposition model: physical concepts and formulation, *J. Geophys. Res.*, 92, 14681–14700, doi:10.1029/JD092iD12p14681, 1987.
- Chaumerliac, N., Leriche, M., and Audiffren, N.: Modeling of scavenging processes in clouds: some remaining questions about the partitioning of gases among gas and liquid phases, *Atmos. Res.*, 53, 29–43, doi:10.1016/S0169-8095(99)00041-1, 2000.
- Damian, V., Sandu, A., Damian, M., Potra, F., and Carmichael, G. R.: The Kinetic PreProcessor KPP – A software environment for solving chemical kinetics, *Comput. Chem. Eng.*, 26, 1567–1579, doi:10.1016/S0098-1354(02)00128-X, 2002.
- Djouad, R., Michelangeli, D. V., and Gong, W.: Numerical solution for atmospheric multiphase models: testing the validity of equilibrium assumptions, *J. Geophys. Res.*, 108, 4602, doi:10.1029/2002JD002969, 2003.
- Edney, E. O., Kleindienst, T. E., Jaoui, M., Lewandowski, M., Offenberger, J. H., Wang, W., and Claeyss, M.: Formation of 2-methyl tetrols and 2-methylglyceric acid in secondary organic

- aerosol from laboratory irradiated isoprene/NOX/SO₂/air mixtures and their detection in ambient PM_{2.5} samples collected in the eastern United States, *Atmos. Environ.*, 39, 5281–5289, doi:10.1016/j.atmosenv.2005.05.031, 2005.
- Ervens, B.: Modeling the processing of aerosol and trace gases in clouds and fogs, *Chem. Rev.*, 115, 4157–4198, doi:10.1021/cr5005887, 2015.
- Ervens, B., Herckes, P., Feingold, G., Lee, T., Collett, J. L., and Kreidenweis, S. M.: On the drop-size dependence of organic acid and formaldehyde concentrations in fog, *J. Atmos. Chem.*, 46, 239–269, doi:10.1023/A:1026393805907, 2003.
- Ervens, B., Turpin, B. J., and Weber, R. J.: Secondary organic aerosol formation in cloud droplets and aqueous particles (aqSOA): a review of laboratory, field and model studies, *Atmos. Chem. Phys.*, 11, 11069–11102, doi:10.5194/acp-11-11069-2011, 2011.
- Ervens, B., Sorooshian, A., Lim, Y. B., and Turpin, B. J.: Key parameters controlling OH-initiated formation of secondary organic aerosol in the aqueous phase (aqSOA), *J. Geophys. Res.-Atmos.*, 119, 3997–4016, doi:10.1002/2013JD021021, 2014.
- Fahey, K. M. and Pandis, S. N.: Optimizing model performance: variable size resolution in cloud chemistry modeling, *Atmos. Environ.*, 35, 4471–4478, doi:10.1016/S1352-2310(01)00224-2, 2001.
- Fahey, K. M., Pandis, S. N., Collett, J. L., and Herckes, P.: The influence of size-dependent droplet composition on pollutant processing by fogs, *Atmos. Environ.*, 39, 4561–4574, doi:10.1016/j.atmosenv.2005.04.006, 2005.
- Gaston, C. J., Riedel, T. P., Zhang, Z., Gold, A., Surratt, J. D., and Thornton, J. A.: Reactive uptake of an isoprene-derived epoxydiol to submicron aerosol particles, *Environ. Sci. Technol.*, 48, 11178–11186, doi:10.1021/es5034266, 2014.
- Giulianelli, L., Gilardoni, S., Tarozzi, L., Rinaldi, M., Decesari, S., Carbone, C., Facchini, M. C., and Fuzzi, S.: Fog occurrence and chemical composition in the Po valley over the last twenty years, *Atmos. Environ.*, 98, 394–401, doi:10.1016/j.atmosenv.2014.08.080, 2014.
- Gong, W., Stroud, C., and Zhang, L.: Cloud processing of gases and aerosols in air quality modeling, *Atmosphere*, 2, 567–616, doi:10.3390/atmos2040567, 2011.
- Graedel, T. E. and Weschler, C. J.: Chemistry within aqueous atmospheric aerosols and raindrops, *Rev. Geophys.*, 19, 505–539, doi:10.1029/RG019i004p00505, 1981.
- Hansen, D. A., Edgerton, E. S., Hartsell, B. E., Jansen, J. J., Kandasamy, N., Hidy, G. M., and Blanchard, C. L.: The southeastern aerosol research and characterization study: Part 1 – overview, *J. Air Waste Manage.*, 53, 1460–1471, doi:10.1080/10473289.2003.10466318, 2003.
- Henderson, B. H., Akhtar, F., Pye, H. O. T., Napelenok, S. L., and Hutzell, W. T.: A database and tool for boundary conditions for regional air quality modeling: description and evaluation, *Geosci. Model Dev.*, 7, 339–360, doi:10.5194/gmd-7-339-2014, 2014.
- Herckes, P., Marcotte, A. R., Wang, Y., and Collett Jr., J. L.: Fog composition in the Central Valley of California over three decades, *Atmos. Res.*, 151, 20–30, doi:10.1016/j.atmosres.2014.01.025, 2015.
- Herrmann, H., Schaefer, T., Tilgner, A., Styler, S. A., Weller, C., Teich, M., and Otto, T.: Tropospheric aqueous-phase chemistry: kinetics, mechanisms, and its coupling to a changing gas phase, *Chem. Rev.*, 115, 4259–4334, doi:10.1021/cr500447k, 2015.
- Hindmarsh, A. C.: ODEPACK: A systematized collection of ODE solvers, in: *Scientific Computing*, edited by: Stepleman, R. S., North Holland, Amsterdam, 55–64, 1983.
- Isaacman-Van Wertz, G., Yee, L. D., Kreisberg, N. M., Wernis, R., Moss, J. A., Hering, S. V., de Sá, S. S., Martin, S. T., Alexander, M. L., Palm, B. B., Hu, W., Campuzano-Jost, P., Day, D. A., Jimenez, J. L., Riva, M., Surratt, J. D., Viegas, J., Manzi, A., Edgerton, E., Baumann, K., Souza, R., Artaxo, P., and Goldstein, A. H.: Ambient Gas-Particle Partitioning of Tracers for Biogenic Oxidation, *Environ. Sci. Technol.*, 50, 9952–9962, doi:10.1021/acs.est.6b01674, 2016.
- Jacob, D. H.: Chemistry of OH in remote clouds and its role in the production of formic acid and peroxymonosulfate, *J. Geophys. Res.*, 91, 9807–9826, doi:10.1029/JD091iD09p09807, 1986.
- Jimenez, J. L., Canagaratna, M. R., Donahue, N. M., Prevot, A. S. H., Zhang, Q., Kroll, J. H., DeCarlo, P. F., Allan, J. D., Coe, H., Ng, N. L., Aiken, A. C., Docherty, K. S., Ulbrich, I. M., Grieshop, A. P., Robinson, A. L., Duplissy, J., Smith, J. D., Wilson, K. R., Lanz, V. A., Hueglin, C., Sun, Y. L., Tian, J., Laaksonen, A., Raatikainen, T., Rautiainen, J., Vaattovaara, P., Ehni, M., Kulmala, M., Tomlinson, J. M., Collins, D. R., Cubison, M. J., Dunlea, E. J., Huffman, J. A., Onasch, T. B., Alfarra, M. R., Williams, P. I., Bower, K., Kondo, Y., Schneider, J., Drewnick, F., Borrmann, S., Weimer, S., Demerjian, K., Salcedo, D., Cottrell, L., Griffin, R., Takami, A., Miyoshi, T., Hatakeyama, S., Shimojo, A., Sun, J. Y., Zhang, Y. M., Dzepina, K., Kimmel, J. R., Sueper, D., Jayne, J. T., Herndon, S. C., Trimborn, A. M., Williams, L. R., Wood, E. C., Middlebrook, A. M., Kolb, C. E., Baltensperger, U., and Worsnop, D. R.: Evolution of Organic Aerosols in the Atmosphere, *Science*, 326, 1525–1529, doi:10.1126/science.1180353, 2009.
- Kleindienst, T. E., Lewandowski, M., Offenber, J. H., Edney, E. O., Jaoui, M., Zheng, M., Ding, X., and Edgerton, E. S.: Contribution of Primary and Secondary Sources to Organic Aerosol and PM_{2.5} at SEARCH Network Sites, *J. Air Waste Manage.*, 60, 1388–1399, doi:10.3155/1047-3289.60.11.1388, 2010.
- Kreidenweis, S. M., Walcek, C. J., Feingold, G., Gong, W., Jacobson, M. Z., Kim, C., Liu, X., Penner, J. E., Nenes, A., and Seinfeld, J. H.: Modification of aerosol mass and size distribution due to aqueous-phase SO₂ oxidation in clouds: comparisons of several models, *J. Geophys. Res.*, 108, 4213, doi:10.1029/2002JD002673, 2003.
- Lelieveld, J. and Crutzen, P. J.: The role of clouds in tropospheric photochemistry, *J. Atmos. Chem.*, 12, 229–267, doi:10.1007/BF00048075, 1991.
- Lewandowski, M., Piletic, I. R., Kleindienst, T. E., Offenber, J. H., Beaver, M. R., Jaoui, M., Docherty, K. S., and Edney, E. O.: Secondary organic aerosol characterization at field sites across the United States during the spring-summer period, *Int. J. Environ. An. Ch.*, 93, 1084–1103, doi:10.1080/03067319.2013.803545, 2013.
- Lim, H., Carlton, A. G., and Turpin, B. J.: Isoprene forms secondary organic aerosol through cloud processing: model simulations, *Environ. Sci. Technol.*, 39, 4441–4446, doi:10.1021/es048039h, 2005.
- Lin, Y.-H., Zhang, H., Pye, H. O. T., Zhang, Z., Marth, W. J., Park, S., Arashiro, M., Cui, T., Budisulistiorini, S. H., Sexton, K. G.,

- Vizuete, W., Xie, Y., Luecken, D. J., Piletic, I. R., Edney, E. O., Bartolotti, L. J., Gold, A., and Surratt, J. D.: Epoxide as a precursor to secondary organic aerosol formation from isoprene photooxidation in the presence of nitrogen oxides, *P. Natl. Acad. Sci. USA*, 110, 6718–6723, doi:10.1073/pnas.1221150110, 2013.
- Liu, J., Horowitz, L. W., Fan, S., Carlton, A. G., and Levy II, H.: Global in-cloud production of secondary organic aerosols: implementation of a detailed chemical mechanism in the GFDL atmospheric model AM3, *J. Geophys. Res.*, 117, D15305, doi:10.1029/2012JD017838, 2012.
- Martin, L. R.: Kinetic studies of sulfite oxidation in aqueous solution, in: *SO₂, NO, and NO₂ oxidation mechanisms: atmospheric considerations*, edited by: Calvert, J. G., Butterworth Publishers, 63–100, 1984.
- Martin, L. R. and Good, T. W.: Catalyzed oxidation of sulfur dioxide in solution: the iron-manganese synergism, *Atmos. Environ.*, 25, 2395–2399, doi:10.1016/0960-1686(91)90113-L, 1991.
- McNeill, V. F.: Aqueous organic chemistry in the atmosphere sources and chemical processing of organic aerosols, *Environ. Sci. Technol.*, 49, 1237–1244, doi:10.1021/es5043707, 2015.
- McNeill, V. F., Woo, J. L., Kim, D. D., Schwier, A. N., Wannell, N. J., Sumner, A. J., and Barakat, J. M.: Aqueous-phase secondary organic aerosol and organosulfate formation in atmospheric aerosols: a modeling study, *Environ. Sci. Technol.*, 46, 8075–8081, doi:10.1021/es3002986, 2012.
- Nguyen, T. B., Bates, K. H., Crouse, J. D., Schwantes, R. H., Zhang, X., Kjaergaard, H. G., Surratt, J. D., Lin, P., Laskin, A., Seinfeld, J. H., and Wennberg, P. O.: Mechanism of the hydroxyl radical oxidation of methacryloyl peroxyoxynitrate (MPAN) and its pathway toward secondary organic aerosol formation in the atmosphere, *Phys. Chem. Chem. Phys.*, 17, 17914–17926, doi:10.1039/C5CP02001H, 2015.
- Pandis, S. N. and Seinfeld, J. H.: Sensitivity analysis of a chemical mechanism for aqueous-phase atmospheric chemistry, *J. Geophys. Res.*, 94, 1105–1126, doi:10.1029/JD094iD01p01105, 1989.
- Pandis, S. N., Seinfeld, J. H., and Pilinis, C.: Chemical composition differences in fogs and cloud droplets of different sizes, *Atmos. Environ.*, 24, 1957–1969, doi:10.1016/0960-1686(90)90529-V, 1990.
- Philip, S., Martin, R. V., van Donkelaar, A., Lo, J. W.-H., Wang, Y., Chen, D., Zhang, L., Kasibhatla, P. S., Wang, S., Zhang, Q., Lu, Z., Streets, D. G., Bittman, S., and Macdonald, D. J.: Global chemical composition of ambient fine particulate matter for exposure assessment, *Environ. Sci. Technol.*, 48, 13060–13068, doi:10.1021/es502965b, 2014.
- Pye, H. O. T., Pinder, R. W., Piletic, P. R., Xie, Y., Capps, S. L., Lin, Y., Surratt, J. D., Zhang, Z., Gold, A., Luecken, D. J., Hutzell, W. T., Jaoui, M., Offenberg, J. H., Kleindienst, T. E., Lewandowski, M., and Edney, E. O.: Epoxide pathways improve model predictions of isoprene markers and reveal key role of acidity in aerosol formation, *Environ. Sci. Technol.*, 47, 11056–11064, doi:10.1021/es402106h, 2013.
- Pye, H. O. T., Luecken, D. J., Xu, L., Boyd, C. M., Ng, N. L., Baker, K. R., Ayres, B. R., Bash, J. O., Baumann, K., Carter, W. P. L., Edgerton, E., Fry, J. L., Hutzell, W. T., Schwede, D. B., and Shepson, P. B.: Modeling the Current and Future Roles of Particulate Organic Nitrates in the Southeastern United States, *Environ. Sci. Technol.*, 49, 14195–14203, doi:10.1021/acs.est.5b03738, 2015.
- Sander, R.: Modeling atmospheric chemistry: interactions between gas-phase species and liquid cloud/aerosol particles, *Surv. Geophys.*, 20, 1–31, doi:10.1023/A:1006501706704, 1999.
- Sander, R., Baumgaertner, A., Gromov, S., Harder, H., Jöckel, P., Kerkweg, A., Kubistin, D., Regelin, E., Riede, H., Sandu, A., Taraborrelli, D., Tost, H., and Xie, Z.-Q.: The atmospheric chemistry box model CAABA/MECCA-3.0, *Geosci. Model Dev.*, 4, 373–380, doi:10.5194/gmd-4-373-2011, 2011.
- Sandu, A. and Sander, R.: Technical note: Simulating chemical systems in Fortran90 and Matlab with the Kinetic PreProcessor KPP-2.1, *Atmos. Chem. Phys.*, 6, 187–195, doi:10.5194/acp-6-187-2006, 2006.
- Sandu, A., Verwer, J. G., Blom, J. G., Spee, E. J., Carmichael, G. R., and Potra, F. A.: Benchmarking stiff ODE solvers for atmospheric chemistry problems, II: Rosenbrock solvers, *Atmos. Environ.*, 31, 3459–3472, doi:10.1016/S1352-2310(97)83212-8, 1997a.
- Sandu, A., Verwer, J. G., van Loon, M., Carmichael, G. R., Potra, F. A., Dabdub, D., and Seinfeld, J. H.: Benchmarking stiff ODE solvers for atmospheric chemistry problems – I. Implicit vs. explicit, *Atmos. Environ.*, 31, 3151–3166, doi:10.1016/S1352-2310(97)00059-9, 1997b.
- Sarwar, G., Fahey, K., Kwok, R., Gilliam, R. C., Roselle, S. J., Mathur, R., Xue, J., Yu, J. Z., and Carter, W. P. L.: Potential impacts of two SO₂ oxidation pathways on regional sulfate concentrations: Aqueous-phase oxidation by NO₂ and gas-phase oxidation by Stabilized Criegee Intermediates, *Atmos. Environ.*, 68, 186–197, doi:10.1016/j.atmosenv.2012.11.036, 2013.
- Schwartz, S. E.: Mass-transport considerations pertinent to aqueous-phase reactions of gases in liquid-water clouds, in: *Chemistry of Multiphase Atmospheric Systems*, edited by: Jaescheke, W., NATO ASI Series, G6, 415–471, 1986.
- Schwartz, S. E. and Freiberg, J. E.: Mass-transport limitation to the rate of reaction of gases in liquid droplets: application to oxidation of SO₂ in aqueous solutions, *Atmos. Environ.*, 15, 1129–1144, doi:10.1016/0004-6981(81)90303-6, 1981.
- Seigneur, C. and Saxena, P.: A theoretical investigation of sulfate formation in clouds, *Atmos. Environ.*, 22, 101–115, doi:10.1016/0004-6981(88)90303-4, 1988.
- Skamarock, W. C., Klemp, J. B., Dudhia, J., Gill, D. O., Barker, D. M., Duda, M. G., Huang, X.-Y., Wang, W., and Powers, J. G.: A description of the advanced research WRF version 3, NCAR Tech Note NCAR/TN 475 STR, 125 pp., UCAR Communications, 2008.
- US Environmental Protection Agency: Guidance on the use of models and other analyses for demonstrating attainment of air quality goals for ozone, PM_{2.5}, and regional haze, EPA-454/B-07-002, 2007.
- Walcek, C. J. and Taylor, G. R.: A theoretical method for computing vertical distributions of acidity and sulfate production within cumulus clouds, *J. Atmos. Sci.*, 43, 339–355, doi:10.1175/1520-0469(1986)043<0339:ATMFVC>2.0.CO;2, 1986.
- Wonaschuetz, A., Sorooshian, A., Ervens, B., Chuang, P. Y., Feingold, G., Murphy, S. M., de Gouw, J., Warneke, C., and Jonsson, H. H.: Aerosol and gas re-distribution by shallow cumulus clouds: an investigation using airborne measurement, *J. Geophys. Res.*, 117, D17202, doi:10.1029/2012JD018089, 2012.
- Xie, Y., Paulot, F., Carter, W. P. L., Nolte, C. G., Luecken, D. J., Hutzell, W. T., Wennberg, P. O., Cohen, R. C., and Pinder, R. W.:

Understanding the impact of recent advances in isoprene photooxidation on simulations of regional air quality, *Atmos. Chem. Phys.*, 13, 8439–8455, doi:10.5194/acp-13-8439-2013, 2013.

Yin, Y., Parker, D. J., and Carslaw, K. S.: Simulation of trace gas redistribution by convective clouds - Liquid phase processes, *Atmos. Chem. Phys.*, 1, 19–36, doi:10.5194/acp-1-19-2001, 2001.